


EFFICIENT COMPUTATION OF SPARSE AND ROBUST MAXIMUM ASSOCIATION ESTIMATORS

A PREPRINT

 **Pia Pfeiffer** *
 Institute of Statistics and
 Mathematical Methods in Economics
 TU Wien
 pia.pfeiffer@tuwien.ac.at

 **Andreas Alfons**
 Erasmus School of Economics
 Erasmus Universiteit Rotterdam
 alfons@ese.eur.nl

 **Peter Filzmoser**
 Institute of Statistics and
 Mathematical Methods in Economics
 TU Wien
 peter.filzmoser@tuwien.ac.at

February 20, 2024

ABSTRACT

Although robust statistical estimators are less affected by outlying observations, their computation is usually more challenging. This is particularly the case in high-dimensional sparse settings. The availability of new optimization procedures, mainly developed in the computer science domain, offers new possibilities for the field of robust statistics. This paper investigates how such procedures can be used for robust sparse association estimators. The problem can be split into a robust estimation step followed by an optimization for the remaining decoupled, (bi-)convex problem. A combination of the augmented Lagrangian algorithm and adaptive gradient descent is implemented to also include suitable constraints for inducing sparsity. We provide results concerning the precision of the algorithm and show the advantages over existing algorithms in this context. High-dimensional empirical examples underline the usefulness of this procedure. Extensions to other robust sparse estimators are possible.

Keywords Biconvex optimization · Sparse robust canonical correlation · Robust estimation · Penalized canonical correlation

1 Introduction

With the availability of new measurement techniques, various different characteristics can be acquired from one and the same object. As an example from tribology, an engine oil can be investigated with respect to its chemical element composition, spectral information can be derived, or various properties concerning friction and wear of the oil can be measured, including image information of the degradation caused by the oil condition. Another example is biological data, specifically, the association between gene expressions and other variables, such as hepatic fatty acid concentrations related to a specific diet [see, e.g., Martin et al., 2007]. The quantification of the relationships between different data sources can be very informative for a deeper understanding of already established mechanisms as well as for the generation of new hypotheses.

More formally, we are interested in the relationships between a p -dimensional real-valued random vector \mathbf{x} and a q -dimensional real-valued random vector \mathbf{y} . We consider the problem of obtaining coefficient vectors \mathbf{a} and \mathbf{b} such that the linear combinations $\mathbf{a}'\mathbf{x}$ and $\mathbf{b}'\mathbf{y}$ have maximum association, measured by an appropriate measure of association between univariate random variables. A widely applied method for this task is canonical correlation analysis (CCA) [see, e.g., Johnson and Wichern, 2007]. The first canonical correlation coefficient ρ_1 and the first pair of canonical variables $(\mathbf{a}_1, \mathbf{b}_1)$ are defined via the maximization of the correlation coefficient between the two linear combinations [see, e.g.,

*This work was funded by the Austrian COMET-Program (project InTribology1, no. 872176) via the Austrian Research Promotion Agency (FFG) and the federal states of Niederösterreich and Vorarlberg and was carried out at the Austrian Excellence Centre of Tribology (AC2T research GmbH) and the TU Wien. The authors acknowledge TU Wien Bibliothek for financial support through its Open Access Funding Programme.

Johnson and Wichern, 2007], that is,

$$\rho_1 = \max_{\substack{\mathbf{a}, \mathbf{b} \\ \|\mathbf{a}\|=\|\mathbf{b}\|=1}} \text{Corr}(\mathbf{a}'\mathbf{x}, \mathbf{b}'\mathbf{y}), \quad (1)$$

$$(\mathbf{a}_1, \mathbf{b}_1) = \text{argmax}_{\|\mathbf{a}\|=1, \|\mathbf{b}\|=1} \text{Corr}(\mathbf{a}'\mathbf{x}, \mathbf{b}'\mathbf{y}). \quad (2)$$

The k -th canonical correlation coefficient ρ_k and the respective pair of canonical variables $(\mathbf{a}_k, \mathbf{b}_k)$ are obtained similarly as in (1), but under the additional constraint that they are uncorrelated with the previous $k - 1$ directions, for $k \in \{2, \dots, \min(p, q)\}$. Expression (1) can be written in terms of the covariance:

$$\begin{aligned} \max_{\substack{\mathbf{a}, \mathbf{b} \\ \|\mathbf{a}\|=\|\mathbf{b}\|=1}} \text{Corr}(\mathbf{a}'\mathbf{x}, \mathbf{b}'\mathbf{y}) &= \max_{\substack{\mathbf{a}, \mathbf{b} \\ \|\mathbf{a}\|=\|\mathbf{b}\|=1}} \frac{\text{Cov}(\mathbf{a}'\mathbf{x}, \mathbf{b}'\mathbf{y})}{\sqrt{\text{Var}(\mathbf{a}'\mathbf{x})}\sqrt{\text{Var}(\mathbf{b}'\mathbf{y})}} \\ &= \max_{\substack{\mathbf{a}, \mathbf{b} \\ \|\mathbf{a}\|=\|\mathbf{b}\|=1}} \frac{\mathbf{a}'\Sigma_{xy}\mathbf{b}}{\sqrt{\mathbf{a}'\Sigma_{xx}\mathbf{a}}\sqrt{\mathbf{b}'\Sigma_{yy}\mathbf{b}}}, \end{aligned} \quad (3)$$

where $\Sigma_{xx} = \text{Cov}(\mathbf{x})$, $\Sigma_{yy} = \text{Cov}(\mathbf{y})$ and $\Sigma_{xy} = \text{Cov}(\mathbf{x}, \mathbf{y})$. The analytical solution is given by the eigenvectors and eigenvalues of a combination of (inverse) covariance matrices: ρ_i^2 are eigenvalues of $\Sigma_{xx}^{-1}\Sigma_{xy}\Sigma_{yy}^{-1}\Sigma_{yx}$ with normed eigenvectors \mathbf{a}_i , and ρ_i^2 are also eigenvalues of $\Sigma_{yy}^{-1}\Sigma_{yx}\Sigma_{xx}^{-1}\Sigma_{xy}$ with normed eigenvectors \mathbf{b}_i , for $i = 1, \dots, \min(p, q)$ [see, e.g., Johnson and Wichern, 2007].

Classically, the involved covariance matrices are estimated by the sample covariances, and this corresponds to maximizing the Pearson correlation coefficient as measure of association. However, these estimators are sensitive to outlying observations, and the solution is not well-defined in the high-dimensional setting, when more variables than observations are available.

There are several approaches in the literature to derive a robust solution. For the *plug-in approach*, the sample covariance is replaced by a robust estimator of the joint covariance of \mathbf{x} and \mathbf{y} . Croux and Dehon [2002] propose to use the minimum covariance determinant (MCD) estimator [Rousseeuw, 1984, 1985], and they derive influence functions for the canonical correlations and vectors based on this plug-in estimator, revealing their robustness properties. For a broader class of affine equivariant scatter and shape matrices, influence functions and limiting distributions of canonical correlations and vectors have been studied by Taskinen et al. [2006]. Langworthy et al. [2020] present theoretical results about using the transformed Kendall correlation, which is more robust under violation of the normality assumption, for the estimation of a scatter matrix.

Another approach is to generalize (1) to a wider class of association estimators. Alfons et al. [2016a] define the optimization problem (1) in a robust way, and also consider rank-correlation measures such as the Spearman rank correlation. In that way, the search for linear relationships, as done with the Pearson correlation, is extended to looking for non-linear relationships. Results concerning Fisher consistency and the influence function underline the good theoretical properties of the corresponding robust maximum association measures, which represent the strongest association between linear combinations of two sets of random variables. The optimization is done using a grid algorithm [Alfons et al., 2016b] which, however, has its limitations concerning the dimensionality p and q of the two random variables.

The high-dimensional case, when more variables than observations are present, is another scenario where the sample covariance matrix performs poorly. This can be addressed by regularizing the covariance matrix as in the penalized matrix decomposition (PMD) method of Witten et al. [2009], where the relationship between the singular value decomposition (SVD) and the Frobenius norm is exploited and optimization is done via a soft-thresholded power method. Chen et al. [2013] develop a canonical pair model and a sparse power algorithm combined with iterative thresholding is applied to estimate the precision matrices. The *alternating regression approach* [Waaaijenborg et al., 2008, Wilms and Croux, 2015a] avoids the computation of covariance matrices and considers problem (1) from a predictive point of view. Wilms and Croux [2015a] derive sparse directions by applying sparsity-inducing regression estimators like the least absolute shrinkage and selection operator (LASSO) [Tibshirani, 1996] or its robustification, sparse least trimmed squares (sparseLTS), introduced by Alfons et al. [2013]. Gu and Wang [2020] combine the alternating regression approach with an alternating direction method of multipliers (ADMM) algorithm for an $L1$ penalized setting, and Shu et al. [2020] describe a CCA method suitable for high-dimensional data based on methods identifying common and distinctive components such as joint and individual variation explained (JIVE) or simultaneous component analysis with rotation to common and distinctive components (DISCO-SCA).

To the best of our knowledge, the only robust *and* sparse method that does not require the repeated computation and inversion of high-dimensional covariance matrices is based on alternating regressions [Wilms and Croux, 2015b].

For higher-order associations, however, there is no efficient implementation available. Several authors propose to use *deflated data matrices* for computing higher-order correlations [Alfons et al., 2016a, Wilms and Croux, 2015b]. However, this approach requires solving several regression problems and can potentially destroy sparsity. Wilms and Croux [2015b] address this by applying a sparsity-inducing regression estimator.

The optimization problems (1)–(3) based on robust correlation or estimators of the covariance matrix lead to highly non-convex objective functions. To obtain a problem formulation that is easier to optimize, the robust estimation and the optimization are *decoupled*: In the first step, the covariance is estimated robustly. This estimator of the covariance matrix is then plugged into the subsequent problem formulation, yielding a biconvex problem. Sparsity can be introduced by adding appropriate constraints. Witten et al. [2009] suggest a similar formulation of the optimization problem for the non-robust case, and an iterative method is presented. Our method, however, also considers the denominator in (3), and offers flexibility in the choice of sparsity constraints as well as for the estimator of the covariance matrix. Since rank-based estimators of the covariance matrix will be considered as well, we will use the terminology “(robust) association measure” instead of “canonical correlation coefficient”, and simply “linear combinations” instead of “canonical vectors” in the following.

The remainder of the paper is organized as follows: First, the reformulation of the problem is detailed, and an appropriate algorithm for its numerical solution is introduced. Then, the results of a simulation study are presented to illustrate the suitability of our approach for a high-dimensional setting with outliers and to compare its performance to existing approaches. We conclude with an outlook on other common statistical tasks that can be solved by applying the algorithm in a similar way.

2 Robust and sparse maximum association

2.1 Formulation as a constrained optimization problem

The optimization problems stated in Section 1 can also be formulated as constrained optimization problem [see, e.g., Anderson, 1958]. This problem formulation has the advantage that the conditions for uncorrelatedness for directions of higher order and sparsity-inducing penalty terms can be stated directly and added as constraints. Starting from expression (3), Σ_{xx} , Σ_{yy} , and Σ_{xy} are substituted with suitable estimators for the covariance, denoted by C_{xx} , C_{yy} , and C_{xy} . Then, the first order maximum association coefficient ρ_1 and the corresponding vectors $(\mathbf{a}_1, \mathbf{b}_1)$ can be obtained as a solution to the following optimization problem:

$$\min_{\mathbf{a} \in \mathbb{R}^p, \mathbf{b} \in \mathbb{R}^q} -F(\mathbf{a}, \mathbf{b}) \quad (4)$$

with $F : \mathbb{R}^p \times \mathbb{R}^q \rightarrow \mathbb{R} : F(\mathbf{a}, \mathbf{b}) = \mathbf{a}' C_{xy} \mathbf{b}$ under the constraints

$$\mathbf{a}' C_{xx} \mathbf{a} = 1, \quad (5)$$

$$\mathbf{b}' C_{yy} \mathbf{b} = 1. \quad (6)$$

This problem formulation avoids the repeated evaluation of the correlation measure that is needed for a projection-pursuit approach as suggested by Alfons et al. [2016a]. The covariance needs to be estimated only once and is then fixed for the optimization process. For higher-order coefficients ρ_k and vectors $(\mathbf{a}_k, \mathbf{b}_k)$, $k \in \{2, \dots, \min(p, q)\}$, constraints for uncorrelatedness with the lower-order directions are needed:

$$\mathbf{a}'_k C_{xx} \mathbf{a}_i = 0, \quad i = 1, \dots, k-1, \quad (7)$$

$$\mathbf{b}'_k C_{yy} \mathbf{b}_i = 0, \quad i = 1, \dots, k-1. \quad (8)$$

Especially for the high-dimensional setting, where p and/or q are big, it can be desirable to set some coefficients to zero in the vectors for the linear combinations. Thus, penalty terms can be added as further constraints in the form of

$$P_{\mathbf{a}_k}(\mathbf{a}_k) \leq c_{\mathbf{a}_k}, \quad (9)$$

$$P_{\mathbf{b}_k}(\mathbf{b}_k) \leq c_{\mathbf{b}_k}, \quad (10)$$

where $c_{\mathbf{a}_k}$ and $c_{\mathbf{b}_k}$ denote positive constants. Here, the penalty terms (9)–(10) are taken as elastic net penalties

$$P_{\mathbf{a}_k}(\mathbf{u}) = \alpha_{\mathbf{a}_k} \|\mathbf{u}\|_1 + (1 - \alpha_{\mathbf{a}_k}) \|\mathbf{u}\|_2, \quad (11)$$

$$P_{\mathbf{b}_k}(\mathbf{u}) = \alpha_{\mathbf{b}_k} \|\mathbf{u}\|_1 + (1 - \alpha_{\mathbf{b}_k}) \|\mathbf{u}\|_2, \quad (12)$$

but other (convex) penalties are also applicable.

Witten et al. [2009] also suggest formulating CCA as an optimization problem and derive the canonical directions via an iterative power method. Our approach is more general in that (i) there are no additional assumptions imposed on the covariance, and (ii) the penalty function can be adapted for each order and can also differ for \mathbf{a} and \mathbf{b} .

2.2 Robust estimation of the covariance matrix

The choice of a suitable estimator of the covariance matrix is crucial for obtaining robust estimators of the canonical vectors [Alfons et al., 2016a]. The robustness of the estimator of the covariance matrix and its stability in the high-dimensional case will influence the respective properties of the resulting coefficients and vectors [Taskinen et al., 2006]. In this work, the focus is on the following estimators: For a base result, the sample covariance matrix is used to estimate Σ_{xx} , Σ_{yy} , and Σ_{xy} , which corresponds to using the Pearson correlation coefficient as measure of association. To achieve robustness and to allow for the high-dimensional case, the minimum regularized covariance determinant (MRCD) [Boudt et al., 2020] and orthogonalized Gnanadesikan-Kettenring (OGK) [Maronna and Zamar, 2002] estimators are used to estimate the joint covariance matrix of \mathbf{x} and \mathbf{y} , which is afterward decomposed into the matrices \mathbf{C}_{xx} , \mathbf{C}_{yy} , and \mathbf{C}_{xy} . The MRCD estimator is based on minimizing the determinant of a *regularized* covariance matrix over all possible subsets of a given size $h \leq n$, and it can also be seen as a robust version of the Ledoit-Wolf estimator [Ledoit and Wolf, 2004]. The OGK estimator relies on applying the identity $\text{Cov}(x, y) = (\sigma(x + y)^2 - \sigma(x - y)^2)/4$, where σ is the standard deviation and x and y denotes a pair of random variables. This identity is applied for the pairwise combinations of the components in the joint vector of \mathbf{x} and \mathbf{y} , by using a robust scale estimator. The final robust estimator of the covariance matrix is obtained after an orthogonalization step. Note that this result is not necessarily positive definite and eigenvalue correction to obtain a positive definite estimator of the covariance matrix is applied. For both the MRCD and the OGK estimator, the implementations in the package `rrcov` [Todorov and Filzmoser, 2009] for the statistical computing environment R [R Core Team, 2022] are used. The OGK estimator is thereby applied with the default settings (using the initial covariance as proposed by Gnanadesikan and Kettenring [1972] and the τ scale [Yohai and Zamar, 1988] for univariate location and dispersion). For MRCD, the size of the h subset, controlled by the parameter α , is set to 75% of the number of observations.

As an alternative, pairwise correlation estimators based on Spearman's rank and Kendall's *tau* are also investigated. They can easily be computed in the high-dimensional case as well and have desirable robustness properties [Croux and Dehon, 2010, Alfons et al., 2016a]. Denote \mathbf{R} as the resulting correlation matrix of the joint vector of $\mathbf{x} = (x_1, \dots, x_p)'$ and $\mathbf{y} = (y_1, \dots, y_q)'$, and $\mathbf{D} = \text{diag}(\sigma(x_1), \dots, \sigma(x_p), \sigma(y_1), \dots, \sigma(y_q))$, where σ corresponds to a (robust) scale estimate. Then the joint covariance is obtained as $\mathbf{D}\mathbf{R}\mathbf{D}$. For σ we used the median absolute deviation (MAD). Note

that for asymptotic normality, it is necessary to apply the transformation $s_{ij} = \frac{6}{\pi} \arcsin\left(\frac{r_{ij}^S}{2}\right)$ to the raw Spearman's rank correlation coefficient r_{ij}^S , and the transformation $\tau_{ij} = \frac{2}{\pi} \arcsin(r_{ij}^K)$ to the raw Kendall's *tau* coefficient r_{ij}^K , where the indices i and j refer to a pair of univariate variables. As Langworthy et al. [2020] point out, a potential issue with those covariance matrices based on pairwise estimation is that they are not necessarily positive definite. Various methods have been proposed to adjust the estimated covariance matrix so that it is positive definite. Rousseeuw and Molenberghs [1993], for example, discuss transformations based on shrinkage and eigenvalues. Higham [2002] presents a method to find the nearest correlation matrix in the Frobenius norm. This algorithm is implemented as the function `nearPD()` in the R package `Matrix` [Bates et al., 2023]. While the positive definiteness of the estimator of the covariance matrix is necessary for the existence of a solution, the presented algorithm does not rely on this property for the computation of the maximum association and corresponding linear combinations. However, the results may not be reliable and in our implementation of the proposed algorithm in the R package `RobSparseMVA` (see Section 3 for more information), it is possible to include a check for positive definiteness and apply the `nearPD()` transformation in case the assumption is violated before starting the optimization algorithm.

2.3 Lagrangian formulation

The Lagrangian function related to the optimization problem (4)–(10) is given by

$$\mathcal{L}(\mathbf{a}, \mathbf{b}, \boldsymbol{\lambda}) = -\mathbf{a}'\mathbf{C}_{xy}\mathbf{b} + \boldsymbol{\lambda}' \cdot H(\mathbf{a}, \mathbf{b}), \quad (13)$$

while the constraints are given by

$$H : \mathbb{R}^p \times \mathbb{R}^q \rightarrow \mathbb{R}^{2k+2} : H(\mathbf{a}, \mathbf{b}) = \begin{cases} \mathbf{a}'\mathbf{C}_{xx}\mathbf{a} - 1 \\ \mathbf{b}'\mathbf{C}_{yy}\mathbf{b} - 1 \\ P_1(\mathbf{a}) - c_a \\ P_2(\mathbf{b}) - c_b \\ \mathbf{a}'\mathbf{C}_{xx}\mathbf{a}_{1:(k-1)} \\ \mathbf{b}'\mathbf{C}_{yy}\mathbf{b}_{1:(k-1)} \end{cases}. \quad (14)$$

For obtaining the first order association coefficients and vectors, the Lagrange multipliers are $\boldsymbol{\lambda} = (\lambda_1, \dots, \lambda_4)'$, and by setting the derivative of \mathcal{L} to $\mathbf{0}$, we obtain

$$-\mathbf{C}_{xy}\mathbf{b} + \lambda_1\mathbf{C}_{xx}\mathbf{a} + \lambda_3\frac{\partial}{\partial\mathbf{a}}P_{\mathbf{a}_1}(\mathbf{a}) = \mathbf{0}, \quad (15)$$

$$-\mathbf{C}_{xy}\mathbf{a} + \lambda_2\mathbf{C}_{yy}\mathbf{b} + \lambda_4\frac{\partial}{\partial\mathbf{b}}P_{\mathbf{b}_1}(\mathbf{b}) = \mathbf{0}. \quad (16)$$

When $P_{\mathbf{a}_k}$ and $P_{\mathbf{b}_k}$ are given as elastic net penalties, the derivatives can be written as

$$\frac{\partial}{\partial\mathbf{u}}P(\mathbf{u}) = \alpha\mathbf{M}_1\mathbf{u} + (1 - \alpha)\mathbf{M}_2\mathbf{u} \quad (17)$$

with $\mathbf{M}_1 = \text{diag}(1/|u_1|, \dots, 1/|u_p|)$ for $\mathbf{u} \in \mathbb{R}^p$ and $\mathbf{M}_2 = 1/\|\mathbf{u}\|_2\mathbf{I} = c\mathbf{I}$. The derivatives of the penalty function do not exist at entries $u_i = 0$. Then, the *subgradient* at this point is used instead. Let $\mathbf{M}_u := \alpha\mathbf{M}_1 + (1 - \alpha)\mathbf{M}_2$ denote the resulting matrix. For a function $f: \mathbb{R}^p \rightarrow \mathbb{R}$, the *subgradient* at $\mathbf{x} \in \text{dom}f$ is defined as the set of vectors $\mathbf{g} \in \mathbb{R}^p$, such that for all $\mathbf{z} \in \text{dom}f$, there holds: $f(\mathbf{z}) \geq f(\mathbf{x}) + \mathbf{g}'(\mathbf{z} - \mathbf{x})$. In the present case, f corresponds to the absolute value function and $\mathbf{g} \in [-1, 1]^{p+q}$ for $\mathbf{x} = \mathbf{0}$ [see, e.g., Boyd and Vandenberghe, 2004].

Substitution in Equations (15) and (16) followed by applying an inverse transformation yields

$$\left[\mathbf{C}_{xx} + \frac{\lambda_3}{\lambda_1}\mathbf{M}_a\right]^{-1}\mathbf{C}_{xy}\left[\mathbf{C}_{yy} + \frac{\lambda_4}{\lambda_2}\mathbf{M}_b\right]^{-1}\mathbf{C}_{yx}\mathbf{a} = \lambda_1\lambda_2\mathbf{a}, \quad (18)$$

$$\left[\mathbf{C}_{yy} + \frac{\lambda_4}{\lambda_2}\mathbf{M}_b\right]^{-1}\mathbf{C}_{yx}\left[\mathbf{C}_{xx} + \frac{\lambda_3}{\lambda_1}\mathbf{M}_a\right]^{-1}\mathbf{C}_{xy}\mathbf{b} = \lambda_1\lambda_2\mathbf{b}. \quad (19)$$

It can be seen that in the case of an L_2 penalty on \mathbf{a} or \mathbf{b} , respectively, this formulation corresponds to a regularization of the estimators of the covariance matrix \mathbf{C}_{xx} and \mathbf{C}_{yy} .

An optimization problem is feasible if there exists at least one point that satisfies the constraints of the problem. In the following we show that with an appropriate choice of the sparsity parameters c_{a_k} and c_{b_k} , the stated optimization is feasible, implying that a solution exists. Let $\Omega \subset \mathbb{R}^p \times \mathbb{R}^q$ denote the set of points that satisfy the constraints (5)–(10). To show that $\Omega \neq \emptyset$, first note that \mathbf{C}_{xx} and \mathbf{C}_{yy} are positive definite matrices that induce a norm on \mathbb{R}^p and \mathbb{R}^q , respectively. Constraints (5) and (7) are fulfilled by any basis of \mathbb{R}^p that is orthonormal with respect to the norm induced by \mathbf{C}_{xx} . The same argument can be applied to constraints (6) and (8) with the norm induced by \mathbf{C}_{yy} . From the equivalence of norms, it follows that there exists a positive constant $c_{a_k} \in \mathbb{R}$ such that $1/c_{a_k}P_{\mathbf{a}_k}(\mathbf{a}_k) \leq 1 = \|\mathbf{a}_k\|_{\mathbf{C}_{xx}}$, and a positive constant $c_{b_k} \in \mathbb{R}$ such that $1/c_{b_k}P_{\mathbf{b}_k}(\mathbf{b}_k) \leq 1 = \|\mathbf{b}_k\|_{\mathbf{C}_{yy}}$.

It follows that the optimization problem (4)–(6) attains a global minimum over Ω : The function F in (4) is continuous and the feasible region $\Omega \subset \mathbb{R}^p \times \mathbb{R}^q$ is non-empty and compact. Then by Weierstrass' theorem, the function F attains a global minimum over Ω .

3 Algorithm

The conditions (5)–(6) in the constrained optimization problem (4)–(10) are not convex. However, they can be modified to be convex by replacing the equality with an inequality constraint:

$$\mathbf{a}'\mathbf{C}_{xx}\mathbf{a} \leq 1 \quad (5a)$$

$$\mathbf{b}'\mathbf{C}_{yy}\mathbf{b} \leq 1. \quad (6a)$$

The modified optimization problem is now biconvex (that is, convex in \mathbf{a} if \mathbf{b} is fixed and vice versa) and has, under the condition that the constants c_{a_k} and c_{b_k} are chosen such that $\mathbf{a}'\mathbf{C}_{xx}\mathbf{a} \geq 1$ and $\mathbf{b}'\mathbf{C}_{yy}\mathbf{b} \geq 1$ hold, the same solution as the original problem [see, e.g., Boyd and Vandenberghe, 2004], as cited by Witten et al. [2009].

Using the *augmented Lagrangian* or *method of multipliers (MM)* [see, e.g., Boyd and Vandenberghe, 2004], the problem can be rewritten as a minimization problem in an unconstrained form. The MM-algorithm has been studied extensively by Bertsekas [1996], and the ADMM variation has been brought back more recently due to its potential for distributed computing [Boyd et al., 2011]. The main idea of the MM approach is to convert the constrained optimization problem to a series of unconstrained problems. The augmented Lagrangian function is given by

$$\mathcal{L}_c(\mathbf{a}, \mathbf{b}, \boldsymbol{\lambda}) = -F(\mathbf{a}, \mathbf{b}) + \boldsymbol{\lambda}' \cdot H(\mathbf{a}, \mathbf{b}) + \frac{c}{2}\|H(\mathbf{a}, \mathbf{b})\|_2^2, \quad (20)$$

Algorithm 1 Sparse and robust maximum association

```

1: Estimate covariance matrices  $C_{xx}, C_{yy}, C_{xy}$ 
2: Initialize  $\mathbf{a}_k^0$  and  $\mathbf{b}_k^0$ 
3: for  $k = 1, 2, \dots, \min(p, q)$  do
4:    $\boldsymbol{\lambda}^0 \leftarrow H(\mathbf{a}_k^0, \mathbf{b}_k^0, \mathbf{a}_{1:(k-1)}, \mathbf{b}_{1:(k-1)})$ 
5:   while  $\|\boldsymbol{\lambda}^{t+1} - \boldsymbol{\lambda}^t\| > \delta$  do
6:      $(\mathbf{a}_k^{t+1}, \mathbf{b}_k^{t+1}) \leftarrow \operatorname{argmin} \mathcal{L}_c(\mathbf{a}_k^t, \mathbf{b}_k^t; \boldsymbol{\lambda}^t)$ 
7:      $\boldsymbol{\lambda}^{t+1} \leftarrow \boldsymbol{\lambda}^t + cH(\mathbf{a}_k^{t+1}, \mathbf{b}_k^{t+1})$ 
8:     if  $0.25 \cdot |H(\mathbf{a}_k^t, \mathbf{b}_k^t)| < |H(\mathbf{a}_k^{t+1}, \mathbf{b}_k^{t+1})|$  then
9:        $c \leftarrow 10 \cdot c$ 
10:    end if
11:     $t \leftarrow t + 1$ 
12:  end while
13: end for

```

where F denotes the primal objective. The constraints are given by

$$H : \mathbb{R}^p \times \mathbb{R}^q \rightarrow \mathbb{R}^{2k+2} : H(\mathbf{a}, \mathbf{b}) = \begin{cases} \mathbf{a}' C_{xx} \mathbf{a} - 1 \\ \mathbf{b}' C_{yy} \mathbf{b} - 1 \\ \mathbf{a}' C_{xx} \mathbf{a}_{1:(k-1)} \\ \mathbf{b}' C_{yy} \mathbf{b}_{1:(k-1)} \\ P_1(\mathbf{a}) - c_a \\ P_2(\mathbf{b}) - c_b \end{cases}. \quad (21)$$

The corresponding Lagrange multipliers are denoted by $\boldsymbol{\lambda} \in \mathbb{R}^{2k+2}$, and the strength of the regularization term for the equality constraints is given by $c \in \mathbb{R}$. This problem can be solved iteratively: in an alternating fashion, first \mathbf{a} and \mathbf{b} are updated, then the dual variable $\boldsymbol{\lambda}$ is updated. The resulting algorithm for the sparse and robust maximum association procedure is provided in Algorithm 1.

As the solution to the minimization problem in line 6 of Algorithm 1 cannot be derived analytically in the general case, the minimization is done by adaptive gradient descent as introduced by Kingma and Ba [2015] and refined by Reddi et al. [2018]. The minimization step is done using the AMSGrad optimizer, given in Algorithm 2 and implemented in the R package `torch` [Falbel and Luraschi, 2023]. The maximum and division in lines 7 and 8, respectively, are executed element-wise, and in the thresholding step in lines 15–16, a_{k_j} and b_{k_j} refer to the components of \mathbf{a}_k and \mathbf{b}_k , respectively.

Other gradient-based optimizers could also be applied. Methods using an adaptive learning rate and momentum such as AMSGrad or Adam are preferred choices, as they are capable of escaping local optima and are less sensitive to the initial choice of the learning rate α_0 . All constraints are subdifferentiable (i.e., for all points in the domain of \mathcal{L}_c , at least one subgradient exists), and the subgradient update as implemented in `torch` can be executed. In addition, a thresholding step is included in the algorithm (lines 15–16) to get true sparsity, which is not possible from the subgradient update alone. Thresholding is done using the moving average of the last M step sizes; in practice we were successful with setting $M = 10$. Depending on the current value of H , the regularization parameter c is updated in lines 8–9 of Algorithm 1. The constants 0.25 and 10 in lines 8–9 were already proposed by Bertsekas [1996] and work well in our simulations.

Biconvex optimization problems are commonly treated in an alternating manner, for the problem (4)–(10) that would suggest updating \mathbf{a} while fixing \mathbf{b} and vice versa (this course of action would correspond to the ADMM algorithm). Even though the partial problems are convex, in general, there is no guarantee that the ADMM converges to the global (or even local) optimum in this case. Therefore, instead of alternating the updates of \mathbf{a} and \mathbf{b} , we propose to perform the update at the same time with a gradient-descent-type algorithm. This way, the algorithm converges towards a solution that satisfies the necessary optimality condition of the Lagrange function \mathcal{L}_0 : via gradient-descent, we are able to identify a stationary point of $\mathcal{L}_c(\mathbf{a}_k^t, \mathbf{b}_k^t; \boldsymbol{\lambda}^t)$, denoted by $(\mathbf{a}_k^{t+1}, \mathbf{b}_k^{t+1})$. This point fulfills $0 \in \nabla \mathcal{L}_c(\mathbf{a}_k^{t+1}, \mathbf{b}_k^{t+1}, \boldsymbol{\lambda}^t) = -\nabla F(\mathbf{a}_k^{t+1}, \mathbf{b}_k^{t+1}) + \boldsymbol{\lambda}^t \nabla H(\mathbf{a}_k^{t+1}, \mathbf{b}_k^{t+1}) + cH(\mathbf{a}_k^{t+1}, \mathbf{b}_k^{t+1}) \nabla H(\mathbf{a}_k^{t+1}, \mathbf{b}_k^{t+1})$. With the update $\boldsymbol{\lambda}^{t+1} = \boldsymbol{\lambda}^t + cH(\mathbf{a}_k^{t+1}, \mathbf{b}_k^{t+1})$, we then have $0 \in \nabla \mathcal{L}_0(\mathbf{a}_k^{t+1}, \mathbf{b}_k^{t+1}; \boldsymbol{\lambda}^{t+1})$.

In the optimization problem derived from classical CCA, only the canonical vectors (of all orders) satisfy the stationarity condition. Theoretically, the algorithm could end up in a stationary point corresponding to the maximum association

Algorithm 2 AMSGrad algorithm [Reddi et al., 2018] for the minimization in line 6 of Algorithm 1, followed by a thresholding step.

```

1: Input  $\mathbf{a}_k^0, \mathbf{b}_k^0$  and  $\eta_{1i}, \eta_2, \alpha_i$ 
2: Initialize  $\mathbf{m}_0 = \mathbf{0}, \mathbf{v}_0 = \mathbf{0}, \hat{\mathbf{v}}_0 = \mathbf{0}$ 
3: while  $\|\nabla_{a,b}\mathcal{L}_c\| > \delta$  do
4:    $\mathbf{g}_i \leftarrow \nabla_{a,b}\mathcal{L}_c$ 
5:    $\mathbf{m}_i \leftarrow \eta_{1i}\mathbf{m}_{i-1} + (1 - \eta_{1i})\mathbf{g}_i$ 
6:    $\mathbf{v}_i \leftarrow \eta_2\mathbf{v}_{i-1} + (1 - \eta_2)\mathbf{g}_i^2$ 
7:    $\hat{\mathbf{v}}_i \leftarrow \max(\hat{\mathbf{v}}_{i-1}, \mathbf{v}_i)$ 
8:    $(\mathbf{a}_k^i, \mathbf{b}_k^i) \leftarrow (\mathbf{a}_k^{i-1}, \mathbf{b}_k^{i-1}) - \alpha_i \frac{\mathbf{m}_i}{\sqrt{\hat{\mathbf{v}}_i}}$ 
9:    $d_a^i \leftarrow \frac{\|\mathbf{a}_k^i - \mathbf{a}_k^{i-1}\|}{\|\mathbf{a}_k^{i-1}\|}$ 
10:   $d_b^i \leftarrow \frac{\|\mathbf{b}_k^i - \mathbf{b}_k^{i-1}\|}{\|\mathbf{b}_k^{i-1}\|}$ 
11:   $i \leftarrow i + 1$ 
12: end while
13:  $\bar{t}_a \leftarrow \text{avg}[d_a^m]_{m=i}^{i-M+1} + 2\text{sd}[d_a^m]_{m=i}^{i-M+1}$ 
14:  $\bar{t}_b \leftarrow \text{avg}[d_b^m]_{m=i}^{i-M+1} + 2\text{sd}[d_b^m]_{m=i}^{i-M+1}$ 
15:  $\mathbf{a}_k \leftarrow [a_{k_j} \text{ if } |a_{k_j}| > \bar{t}_a, 0 \text{ otherwise}]_{j=1}^p$ 
16:  $\mathbf{b}_k \leftarrow [b_{k_j} \text{ if } |b_{k_j}| > \bar{t}_b, 0 \text{ otherwise}]_{j=1}^q$ 

```

and the respective linear combinations of a different order. However, our simulations indicate that this is not a problem in practice, as the applied variant of gradient descent is able to escape local optima.

3.1 Hyperparameter optimization

Another important aspect of the algorithm is the choice of the hyperparameters. The mixing parameters α_{a_k} and α_{b_k} of the elastic net penalties in (11) and (12) are often set in advance by the user, but the sparsity parameters c_{a_k} and c_{b_k} have to be determined in a data-driven manner. Grid search in combination with cross-validation quickly becomes infeasible if the search space becomes larger, especially in more than one dimension. An alternative is *Bayesian optimization* of the given hyperparameters. An introduction to Bayesian optimization for hyperparameter optimization can be found, for example, in Frazier [2018]. The benefit of using Bayesian optimization instead of grid search is that the information from previous function evaluations can be used to determine the best next point to execute the function. This way, a much bigger search space can be covered, and, in addition, it is less likely to miss a good parameter configuration due to the size of the grid. For the basic algorithm, it is assumed that there is a budget of in total N function evaluations. We also need to define a score to be maximized during the hyperparameter optimization, and an appropriate acquisition function. A Gaussian prior is placed on the score function, then its value is observed at n_0 points. Until N iterations are reached, the following steps are repeated: (i) update the posterior probability distribution on the score function, (ii) determine the maximum of the acquisition function, and (iii) observe the score value at this parameter configuration.

We used the implementation in the R package `ParBayesianOptimization` [Wilson, 2022] with the expected improvement as acquisition function and the tradeoff product optimization (TPO) as score function. It is similar to the TPO criterion used by Filzmoser et al. [2022] and models the tradeoff between sparsity in the estimated linear combinations, $\hat{\mathbf{a}}_k$ and $\hat{\mathbf{b}}_k$, and the estimated value $\hat{\rho}_k$ of the robust association measure. Figure 1 illustrates this criterion. The original criterion

$$\text{score} = |\hat{\rho}_k| \cdot \left(2 - \frac{\#\{\hat{\mathbf{a}}_k \neq 0\}}{p} - \frac{\#\{\hat{\mathbf{b}}_k \neq 0\}}{q} \right)$$

where $\#\{\hat{\mathbf{a}}_k \neq 0\}$ returns the number of non-zero components in $\hat{\mathbf{a}}_k$, and similar for $\hat{\mathbf{b}}_k$, can be adapted for non-sparse regularization by including the elastic net parameters α_{a_k} and α_{b_k} :

$$\text{score} = |\hat{\rho}_k| \cdot \left(2 - \alpha_{a_k} \frac{\#\{\mathbf{a}_k \neq 0\}}{p} - \alpha_{b_k} \frac{\#\{\mathbf{b}_k \neq 0\}}{q} \right). \quad (22)$$

Both the sparsity and elastic net parameters can be chosen differently for each k and $\hat{\mathbf{a}}_k$ or $\hat{\mathbf{b}}_k$, respectively. In our simulations, presented in Section 4, the chosen elastic net parameters α_{a_k} and α_{b_k} are assumed to be the same for

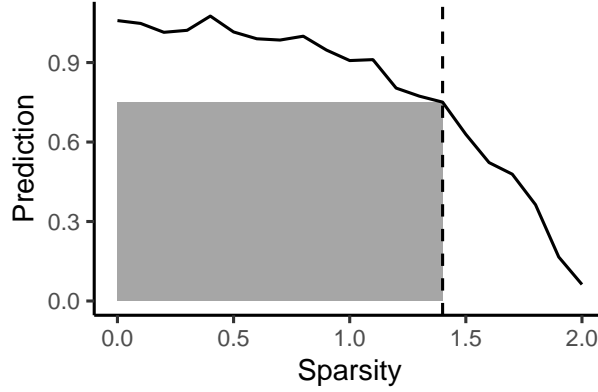


Figure 1: Visualization of the tradeoff product optimization (TPO) criterion (22) used as a score function in Bayesian hyperparameter optimization. The TPO score corresponds to finding the biggest area under the curve of prediction (robust association measure) over sparsity.

each k , while the Bayesian optimization procedure to determine the optimal sparsity parameters is run for each k . Furthermore, Section 4.2.1 of the simulation study is dedicated to the precision of the algorithm, i.e., the performance of the algorithm when the true covariance matrix and theoretically optimal sparsity parameters are provided.

3.2 Initialization

For the presented algorithm, suitable starting values \mathbf{a}_k^0 and \mathbf{b}_k^0 for the linear combinations \mathbf{a}_k and \mathbf{b}_k , respectively, and for the associated Lagrange multiplier λ_k are needed. For the elements of \mathbf{a}_1^0 and \mathbf{b}_1^0 , we use the average contribution of the respective row or column in $\mathbf{C}_{xy} = [c(x_i, y_j)]$ as a starting value,

$$a_{1_i}^0 = \frac{1}{q} \sum_{j=1}^q c(x_i, y_j) \quad \text{for } i = 1, \dots, p, \quad (23)$$

$$b_{1_j}^0 = \frac{1}{p} \sum_{i=1}^p c(x_i, y_j) \quad \text{for } j = 1, \dots, q, \quad (24)$$

and for the Lagrange multipliers, the constraints are evaluated at the starting points,

$$\lambda_k^0 = H(\mathbf{a}_k^0, \mathbf{b}_k^0). \quad (25)$$

If a non-robust estimator of the covariance matrix is used, the starting values may already be influenced by outlying observations. A more detailed investigation of what happens when the number of outlying observations is increased is given in Section 4.2.3.

For the computation of directions of higher order, the concept of "deflated" data matrices is often described in the literature [e.g. Branco et al., 2003]. However, this step can be detrimental to the sparsity in the higher-order vectors. In our approach, constraints for uncorrelatedness to lower-order directions are added to the model. Higher-order directions need to satisfy Equations (7) and (8), respectively. Basically, this means that \mathbf{a}_k is in the left null space of $\mathbf{C}_{xx} \mathbf{a}^{(i:k-1)}$ and \mathbf{b}_k is in the left null space of $\mathbf{C}_{yy} \mathbf{b}^{(i:k-1)}$. These affine constraints preserve the biconvexity and suggest the following variation for determining the starting values for higher-order linear combinations: The orthogonal complements $\mathbf{A}_k^\perp := \{\mathbf{a} : \mathbf{a}' \mathbf{C}_{xx} \mathbf{a}^{(i:k-1)} = 0\}$ and $\mathbf{B}_k^\perp := \{\mathbf{b} : \mathbf{b}' \mathbf{C}_{yy} \mathbf{b}^{(i:k-1)} = 0\}$ are computed, then the starting values \mathbf{a}_k^0 and \mathbf{b}_k^0 are chosen as the orthogonal projections of \mathbf{a}_1^0 and \mathbf{b}_1^0 on \mathbf{A}_k^\perp and \mathbf{B}_k^\perp , respectively.

In our simulations, both the naive approach and this "orthogonal" initialization for the higher-order linear combinations are compared.

4 Simulation study

A simulation study was conducted to compare the performance of the proposed method using different (robust) estimators of the covariance matrix. The comparison is also done with other approaches already mentioned in Section 1,

namely PMD by Witten et al. [2009], and SRAR by Wilms and Croux [2015a]. For PMD, the R package PMA [Witten and Tibshirani, 2020] was used, for SRAR the code available from <https://sites.google.com/view/iwilms/software> was used. Our algorithm is implemented in the R package RobSparseMVA and available online <https://github.com/piapfeiffer/RobSparseMVA>.

A good sparse and robust method should be efficient when the number of variables grows, avoid misidentifying important variables, and should attain these properties in the presence of outliers in the data [see, e.g., Zou et al., 2006, Todorov and Filzmoser, 2013]. In order to check those requirements, the following *performance measures* are used. For measuring accuracy, the angle $\theta_a = \arccos\left(\frac{\mathbf{a}'\hat{\mathbf{a}}}{\|\mathbf{a}\|\|\hat{\mathbf{a}}\|}\right)$ between the true and estimated canonical variables is computed. Note that only the results for one of the linear combinations are presented here as the results for the other are qualitatively similar. The true-positive rate (TPR), corresponding to the rate of correctly identified non-zero components, together with the true-negative rate (TNR), or the rate of correctly identified zero components, measure whether non-zero variables are identified correctly. For studying the scalability, the runtime for a growing number of variables is measured.

For the computation of above performance measures, the true linear combinations \mathbf{a} and \mathbf{b} have to be computed: They can be derived from the true covariance matrices Σ_{xx} , Σ_{xy} , and Σ_{yy} as eigenvectors of $\Sigma_{xx}^{-1}\Sigma_{xy}\Sigma_{yy}^{-1}\Sigma_{yx}$ and $\Sigma_{yy}^{-1}\Sigma_{yx}\Sigma_{xx}^{-1}\Sigma_{xy}$, respectively, see Section 1.

4.1 Simulation design

Different simulation settings and contamination scenarios [similar to Wilms and Croux, 2015b] are considered. Clean data are generated from a multivariate normal distribution: $(\mathbf{x}, \mathbf{y})' \sim \mathcal{N}_{p+q}(\mathbf{0}, \Sigma)$. For the contaminated scenario, $c_r\%$ contamination is generated from a multivariate normal distribution with a mean shift: $(\mathbf{x}, \mathbf{y})' \sim \mathcal{N}_{p+q}(c_s \cdot \mathbf{1}, \Sigma)$, where c_s denotes the contamination strength. To simulate a heavy-tailed distribution, data are generated from a multivariate t-distribution: $(\mathbf{x}, \mathbf{y})' \sim t_3(\mathbf{0}, \Sigma)$. The joint covariance matrix $\Sigma = \begin{bmatrix} \Sigma_{xx} & \Sigma_{xy} \\ \Sigma_{xy}' & \Sigma_{yy} \end{bmatrix}$ is given according to the following simulation settings:

1. Low-dimensional, order 2: $p = q = 10, n = 100$ observations

$$\begin{aligned} \Sigma_{xx} &= \mathbf{I}_{10} \\ \Sigma_{yy} &= \mathbf{I}_{10} \\ \Sigma_{xy} &= \begin{bmatrix} 0.9 & 0 & \mathbf{0}_{1 \times 8} \\ 0 & 0.7 & \mathbf{0}_{1 \times 8} \\ \mathbf{0}_{8 \times 1} & \mathbf{0}_{8 \times 1} & \mathbf{0}_{8 \times 8} \end{bmatrix} \end{aligned}$$

The true associations in this setting are $\rho_1 = 0.9$ and $\rho_2 = 0.7$, and the true linear combinations are $\mathbf{a}_1 = \mathbf{b}_1 = (1, \mathbf{0}_{1 \times 9})'$ and $\mathbf{a}_2 = \mathbf{b}_2 = (0, 1, \mathbf{0}_{1 \times 8})'$.

2. High-dimensional, order 2: $p = q = 100, n = 50$ observations

$$\begin{aligned} \Sigma_{xx} &= \begin{bmatrix} \mathbf{S}_{10 \times 10}^1 & \mathbf{0}_{10 \times 10} & \mathbf{0}_{10 \times 80} \\ \mathbf{0}_{10 \times 10} & \mathbf{S}_{10 \times 10}^2 & \mathbf{0}_{10 \times 80} \\ \mathbf{0}_{80 \times 10} & \mathbf{0}_{80 \times 10} & \mathbf{I}_{80 \times 80} \end{bmatrix} \\ \Sigma_{yy} &= \Sigma_{xx} \\ \Sigma_{xy} &= \begin{bmatrix} \mathbf{0.9}_{10 \times 10} & \mathbf{0}_{10 \times 10} & \mathbf{0}_{10 \times 80} \\ \mathbf{0}_{10 \times 10} & \mathbf{0.5}_{10 \times 10} & \mathbf{0}_{10 \times 80} \\ \mathbf{0}_{80 \times 10} & \mathbf{0}_{80 \times 10} & \mathbf{0}_{80 \times 80} \end{bmatrix} \end{aligned}$$

where $\mathbf{S}_{ij}^1 = 1$ if $i = j$ and $\mathbf{S}_{ij}^1 = 0.9$ for $i \neq j$ and $\mathbf{S}_{ij}^2 = 1$ if $i = j$ and $\mathbf{S}_{ij}^2 = 0.7$ for $i \neq j$. The true associations in this setting are $\rho_1 = 0.989$ and $\rho_2 = 0.685$, and the true linear combinations are $\mathbf{a}_1 = \mathbf{b}_1 = (\mathbf{0.105}_{1 \times 10}, \mathbf{0}_{1 \times 90})'$ and $\mathbf{a}_2 = \mathbf{b}_2 = (\mathbf{0}_{1 \times 10}, \mathbf{0.117}_{1 \times 10}, \mathbf{0}_{1 \times 80})'$.

4.2 Simulation results

4.2.1 Precision of the algorithm

For evaluating the precision of the algorithm, we avoid estimating the covariance matrix but plug in the true covariance matrix Σ into the algorithm. We also compare the precision when the theoretically optimal sparsity parameters are

provided (which can be derived from the true linear combinations (\mathbf{a}, \mathbf{b}) as $c_a = \|\mathbf{a}\|_1$ and $c_b = \|\mathbf{b}\|_1$) and when the sparsity parameters are estimated via Bayesian optimization. The results of these (deterministic) computations are presented in Table 1. For the first-order association measure, the algorithm always converges to the true solution. For higher-order association measures, it can be seen that the sparsity parameters need to be chosen with more care and that the orthogonal start is necessary for the high-dimensional setting. Furthermore, it can be concluded that starting with an orthogonal projection for the second-order directions is beneficial. Therefore, the results of all subsequent simulations are shown for this initialization.

Table 1: Performance measures given the true covariance. The true association measures for the low-dimensional and high-dimensional setting are $\rho_1 = 0.9$ and $\rho_2 = 0.7$, and $\rho_1 = 0.989$ and $\rho_2 = 0.685$, respectively.

Setting	Sparsity	Initialization	Order	Angle θ_a	TPR	TNR	Association
Low-dimensional	known	naive	1	0	1	1	0.9
		naive	2	0	1	0.89	0.7
		orthogonal	2	0	1	1	0.7
	estimated	naive	1	0	1	1	0.9
		naive	2	0	1	0.89	0.7
		orthogonal	2	0	1	1	0.7
High-dimensional	known	naive	1	0	1	1	0.989
		naive	2	1.57	0	0.89	0.989
		orthogonal	2	0.23	1	1	0.683
	estimated	naive	1	0	1	1	0.989
		naive	2	1.57	0	0.89	0.989
		orthogonal	2	0	1	1	0.685

4.2.2 Comparison to other methods

For the given scenarios and settings, the proposed method using different estimators of the covariance matrix is compared to SRAR by Wilms and Croux [2015b] and sparse CCA via PMD by Witten et al. [2009] in terms of estimation accuracy, measured by the angle θ_a , and sparsity control, measured by the TPR and TNR. For our algorithm, we used the orthogonal initialization to compute the second-order association. The naive initialization leads to worse results (not shown here).

The results over 100 repetitions for estimators of the covariance matrix used in our algorithm (left of the dashed line) with SRAR [Wilms and Croux, 2015b] and PMD [Witten et al., 2009] are summarized in Figure 2. The left column presents the results for the low-dimensional setting, the right column for the high-dimensional setting. The different plot symbols encode different contamination scenarios; black presents first-order results, and gray second-order results. Shown are the mean values over 100 repetitions for the metrics, together with error bars representing the standard error range. We present the results for uncontaminated data, for contamination of 5% of the observations with contamination strength $c_s = 2$, and for data generated from a multivariate t_3 distribution, see Section 4.1.

The results for the low-dimensional setting are shown on the left-hand side of Figure 2. The angle, TPR, and TNR are only presented for the estimated canonical variables \mathbf{a}_1 and \mathbf{a}_2 . For the non-contaminated data, the performance across all methods is similar. Estimating the second-order component leads to slightly worse results - with the exception of PMD, where the results are highly precise. The behavior under contamination and heavy tails is still comparable to the non-contaminated case; only SRAR and PMD have problems identifying the correct sparsity. For PMD, this is especially apparent in the figures depicting the TPR and TNR: Both for the first-order and second-order linear combinations, the TNR is 1, but the TPR is only around 0.5, indicating that the resulting linear combinations are too sparse.

For the high-dimensional setting (right-hand side of Figure 2), more differences can be observed: When the data are uncontaminated, our algorithm based on the Pearson correlation is highly accurate. This can be in part attributed to the regularization effect on the estimators of the covariance matrix described in Equations (18)–(19). While the performance for the high-dimensional setting is overall worse, and all methods suffer from a decrease in accuracy for the second-order canonical vectors, it can be observed that for the robust OGK and MRCD estimators, the accuracy level for the second-order component is the same as it already is for the first-order component for SRAR (Figure 2: top-right). Our algorithm with robust estimators of the covariance matrix shows superior performance for the TPR. Especially interesting is the good result for the covariance based on Spearman’s rank and Kendall’s τ in the scenario

using the t-distribution. This finding coincides with the work presented in Langworthy et al. [2020]. The TNR is good for all variants of our algorithm and for PMD in the clean setting. SRAR performs worse, and similarly to the accuracy, the TNR for the second-order components estimated using our algorithm is on the same level as the TNR for SRAR in the first-order components. Difficulties with accuracy and estimating the correct sparsity are also reflected in the resulting association measure.

4.2.3 Increasing contamination

For both the low-dimensional and high-dimensional settings described in Section 4.1, the contamination proportion was increased from $cp = 0\%$ to $cp = 50\%$, and again, the same performance measures were evaluated. The results averaged over 50 repetitions comparing the different robust estimators are shown in Figure 3. On the left side, the performance metrics for the low-dimensional setting are given, on the right side, the results for the high-dimensional setting are shown. The different line types correspond to the performance metrics for our method using different estimators for the covariance matrix (Pearson, Spearman, Kendall, OGK, MRCD) and the sparse and robust alternating regressions (SRAR) technique on the other hand. The results for the penalized matrix decomposition (PMD) are omitted, as it is already affected by a small proportion of outlying observations. While the metrics for accuracy show in the low-dimensional setting an advantage for the alternating regressions approach, the other metrics are comparable across the methods. For the high-dimensional setting, the results are more distinguished: The proposed method outperforms the SRAR approach, while the robustness against an increased contamination proportion depends on the estimator of the covariance matrix. In these plots it is clearly visible that the h -subset parameter for MRCD was set to $\alpha = 0.75$, as the performance gets much worse over a contamination proportion of $cp = 25\%$. The OGK estimator also exhibits interesting behavior: The TPR metric decrease up to a contamination proportion of 40%, then it jumps to 1. The reason can be observed when analyzing the TNR metric: After a contamination proportion of 40% is reached, all components are identified to be non-zero. Another interesting observation is that while for all estimators the performance metrics decline, the predicted association measure still seems to be reliable. The contamination strength (mean shift) was also varied between $c_s = 2$ and $c_s = 10$, but was not found to have an effect on the performance of the different estimators. Therefore, these results are omitted here.

4.2.4 Runtime

For evaluating the runtime, the first-order canonical directions and association were computed using our algorithm and SRAR for increasing dimension $q = 50, \dots, 10000$ while keeping the dimensionality of the other side, $p = 10$, and the number of samples, $n = 100$, fixed. The joint covariance matrix $\Sigma = \begin{bmatrix} \Sigma_{xx} & \Sigma_{xy} \\ \Sigma'_{xy} & \Sigma_{yy} \end{bmatrix}$ is given according to the settings:

$$\begin{aligned} \Sigma_{xx} &= [\mathbf{S}_{10 \times 10}^1] \\ \Sigma_{yy} &= \begin{bmatrix} \mathbf{S}_{10 \times 10}^1 & \mathbf{0}_{10 \times (q-10)} \\ \mathbf{0}_{(q-10) \times 10} & \mathbf{I}_{(q-10) \times (q-10)} \end{bmatrix} \\ \Sigma_{xy} &= \begin{bmatrix} \mathbf{0.8}_{10 \times 10} & \mathbf{0}_{10 \times (q-10)} \\ \mathbf{0}_{(q-10) \times 10} & \mathbf{0}_{(q-10) \times (q-10)} \end{bmatrix} \end{aligned}$$

where $S_{ij}^1 = 1$ if $i = j$ and $S_{ij}^1 = 0.8$ for $i \neq j$.

To remove the effect of the hyperparameter search, fixed optimal sparsity parameters were used for all methods. The results are averaged over 10 replications and presented in Figure 4. The increasing dimension q is shown on the horizontal axis on a log scale, and the CPU runtime of the algorithm is shown on the vertical axis in minutes. It can be observed that the presented algorithm based on adaptive gradient descent has a comparable dependence of runtime to problem size to the only other robust and sparse alternative. However, it is obvious that the runtime heavily depends on the type of association estimator used, as the joint covariance needs to be estimated fully before starting the optimization. The covariance matrix only needs to be estimated once, and if it is already available, gradient descent scales better to high-dimensional data than regression-type algorithms. In combination with pairwise estimators of the covariance matrix, which are also easy to compute in high dimensions, the proposed algorithm could also serve as a more time-efficient alternative to alternating regressions.

In summary, the simulation results demonstrate the comparable or better performance of our proposed method, depending on the contamination scenario. Especially for the high-dimensional scenario, our method in combination with an appropriate estimator for the covariance matrix performs well, also for higher-order directions. When runtime is of concern, the method based on Spearman or Kendall correlation should be considered, as these measures have better

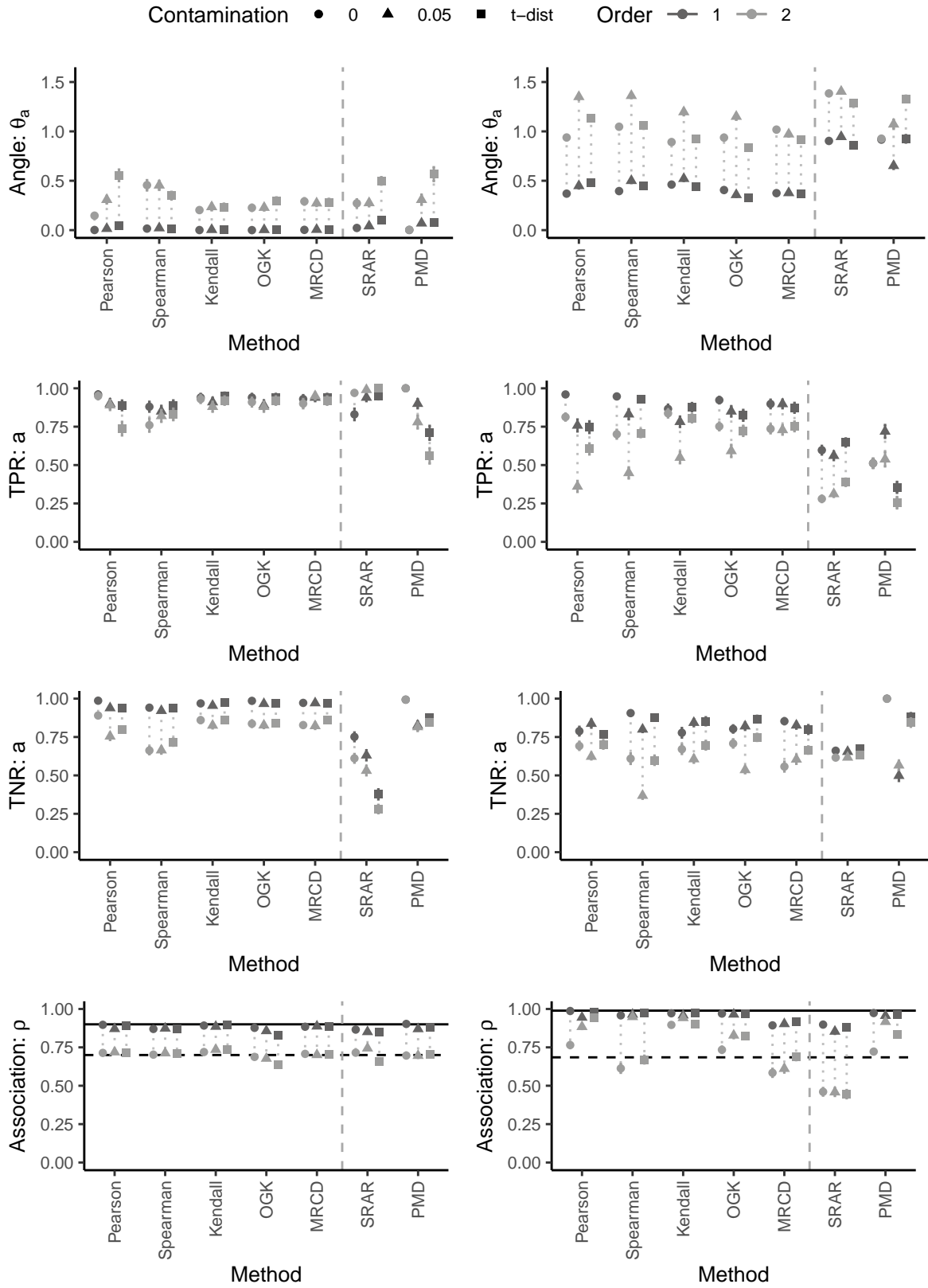


Figure 2: Comparison of performance measures for the different methods.

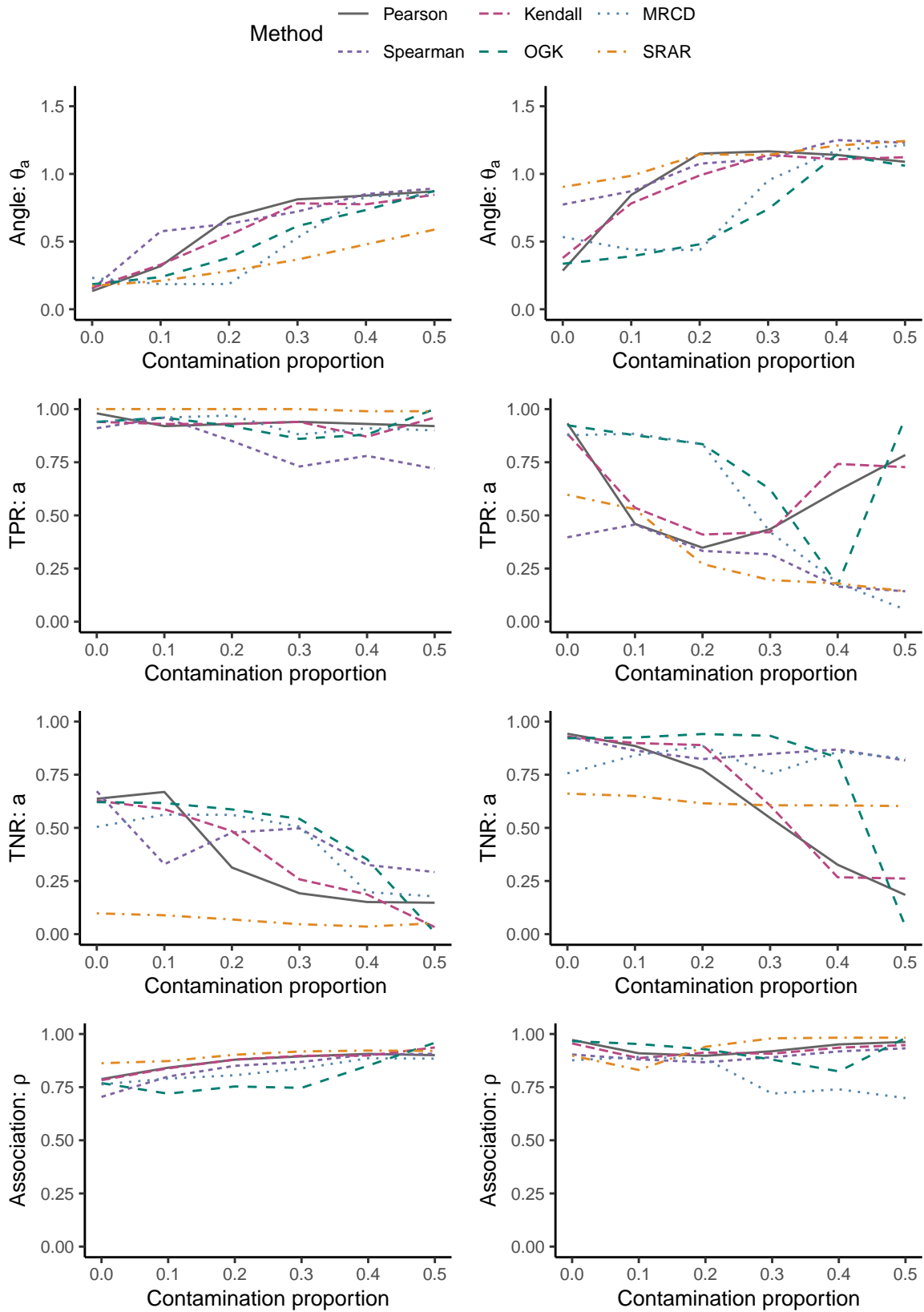


Figure 3: Increasing contamination ratio for different (robust) methods.

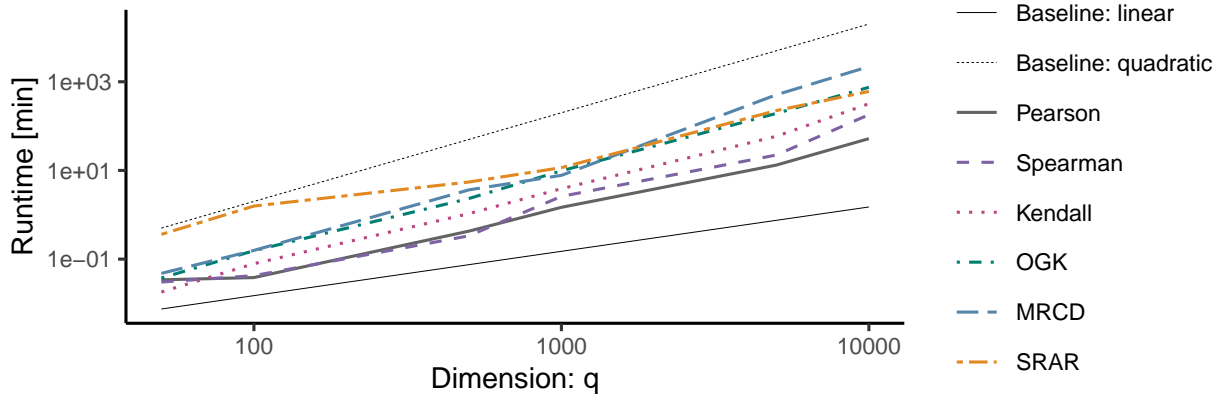


Figure 4: Log-log plot of CPU runtime in minutes versus dimensionality q of second variable.

robustness properties than Pearson correlation, while still being efficient to compute. In general, the OGK estimator seems to be a sensible choice, leading to good performance metrics in both low-dimensional and high-dimensional settings and for an increased contamination ratio.

5 Examples

In this section, the proposed method will be applied to two data sets from different fields: biology and tribology. For both, the number of observations is significantly lower than the number of variables, and the flexibility of choosing the sparsity via the elastic-net penalty for each side is desirable.

In order to compare the performance of classical and robust estimation, we compare the out-of-sample performance of the robust and non-robust estimators by randomly splitting the data into a training and test set and computing the out-of-sample residual score

$$r = \frac{1}{n_{\text{test}}} \frac{1}{n_{\text{rep}}} \sum_{j=1}^{n_{\text{test}}} \sum_{i=1}^{n_{\text{rep}}} \|\mathbf{a}'_{\text{train}_i} \mathbf{x}_j - \mathbf{b}'_{\text{train}_i} \mathbf{y}_j\|^2, \quad (26)$$

where $\mathbf{a}_{\text{train}_i}$ and $\mathbf{b}_{\text{train}_i}$ are the first order linear combinations that are estimated on the i -th training set, n_{test} is the number of test set observations, and \mathbf{x}_j and \mathbf{y}_j are observations from the corresponding test sets. The random training and test splits are repeated n_{rep} times. Since outliers in the test sets could contaminate this residual score measure, we also use a trimmed version, by trimming the largest 10% of all the squared test residuals and dividing by the corresponding number of observations. We also report the (in-sample) association measure, averaged over n_{rep} random training and test splits.

5.1 Application to the nutrimouse dataset

The nutrimouse dataset is publicly available via the CCA package in R [González and Déjean, 2021] and has been discussed in the related literature, for example, by Wilms and Croux [2015b]. It contains $n = 40$ observations of $p = 120$ gene expressions and $q = 21$ concentrations of fatty acids. Martin et al. [2007] provide a detailed description of the dataset, and investigate the influence of a certain diet on numerous gene expressions in mice. In this setting, the goal is to identify a set of genes that has a large association with a set of lipids [cf. Wilms and Croux, 2015b]. The two datasets were robustly centered and scaled with median and MAD before continuing with the analysis. We compare the results of the sparse CCA method by Witten et al. [2009] with the proposed method by computing the residual score r , see Equation (26) in a leave-one-out cross-validation (CV) setting, i.e., the i -th training set consists of all observations except i , and the i -th test set only contains observation i .

The results are given in Table 2: The residual score for the robust method is much lower, the same holds for the trimmed version. The estimated association is 0.76 for PMD and 0.89 for our method using the OGK estimator. Additionally, the contributions to the residual scores for both methods are presented as a scatterplot in Figure 5. Most of the points are above the 45° line, i.e. smaller for the robust method. Similar to Wilms and Croux [2015b] we can conclude that the out-of-sample performance of the robust method is better, and therefore present the estimated linear combinations of this method in Figure 6.

Table 2: Residual scores and association measure based on data splitting for the nutrilogue dataset.

Method	r	r (trimmed)	Association
sparse CCA	2.15	1.10	0.76
OGK	0.49	0.18	0.89

Out of the $p = 120$ gene expressions, 54 are selected by the algorithm, and out of $q = 21$ fatty acids, 16 are selected. Upon comparison with the selected variables presented by Wilms and Croux [2015b], we can identify the following sets of fatty acids that have been selected by both the SRAR method and ours: C.20.1n.9, C.20.2n.6 and C22.4n.6 with the highest (absolute) coefficients. Among the fatty acids related to the diets of the mice, namely C22:6n-3, C22:5n-3, C22:5n-6, C22:4n-3, and C20:5n-3 [see Martin et al., 2007], 5 are selected by our method. For the gene expressions, the coefficient values differ more than for the fatty acids. CYP3A11, which has been found to have a significant influence by Martin et al. [2007], is selected by both methods. The influence of diet on Lpin1 is also discussed by Martin et al. [2007] and has the highest absolute coefficient in our model.

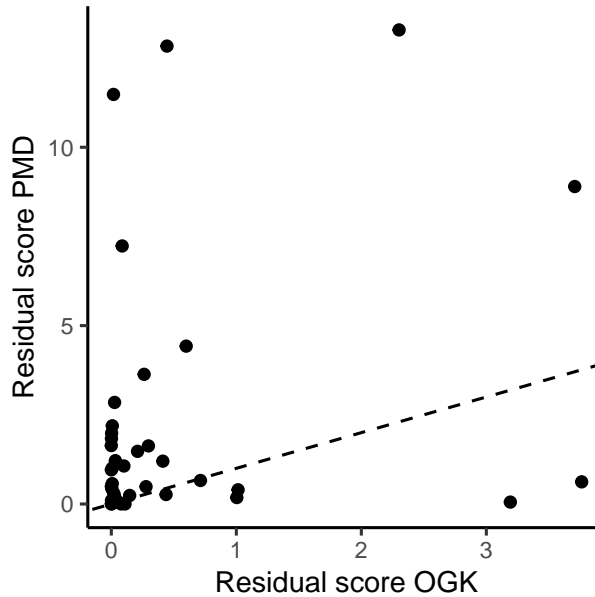


Figure 5: Scatterplot of leave-one-out cross-validation (CV) scores for PMD and the proposed method using the OGK estimator for the nutrilogue dataset. Almost all points are above the 45° line, indicating a better out-of-sample performance for the robust estimator.

5.2 Application in tribology

Fourier-transform infrared spectroscopy (FTIR) spectra to monitor a lubricant’s degradation process and their relation to different indicators for oil condition have been studied by several authors [see, for example, Pfeiffer et al., 2022]. However, the goal is to also understand the association between lubricant chemistry and lubrication performance. Pfeiffer and Filzmoser [2023] demonstrated how features from optical data of wear scar areas can be extracted and used in a robust partial least-squares (PLS) model to relate the wear scar to oil condition, measured by alteration duration.

We demonstrate that by using the method presented in this paper, the two high-dimensional datasets can be associated directly. The dataset consists of $n = 214$ observations, FTIR spectra with $p = 1668$ variables, and HoG (histogram of gradients) feature vectors, with $q = 1836$ variables, representing the wear scar images. As previous studies have shown, while sparsity is beneficial for the evaluation of FTIR spectra, it does not yield good results for HoG image features [Pfeiffer and Filzmoser, 2023]. This example also illustrates the flexibility of our approach, being able to choose a sparsity-inducing penalty on one side, while applying L_2 -regularization on the other. Before proceeding with the analysis (independent from which estimator of the covariance matrix was used), the HoG feature vectors were robustly centered and scaled using median and MAD, respectively.

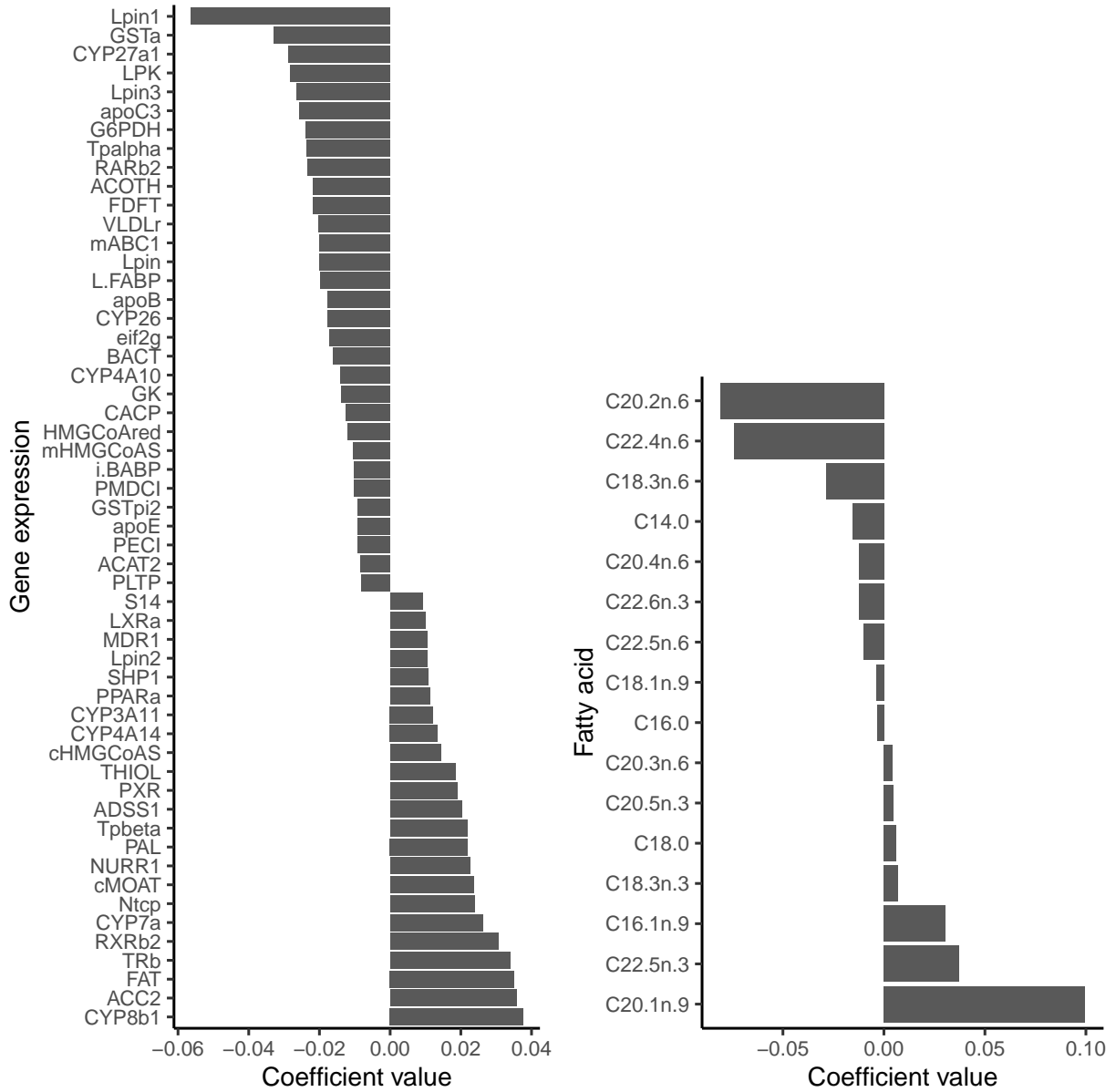


Figure 6: Estimated linear combinations using the OGK estimator of the covariance matrix for the `nutrimouse` dataset.

We compute the residual score, see Equation (26), for a 90%–10% split, repeated 5 times. Here we run the algorithm using the Pearson correlation (sample covariance matrix), and as a robust counterpart we use the OGK estimator of the covariance matrix. The resulting residual scores are given in Table 3. It can be observed that the overall out-of-sample performance for the robust estimator is clearly better than for the classical one, while the estimated association is comparable.

Table 3: Residual scores and association measure based on data splitting for the `tribology` dataset.

Method	r	r (trimmed)	Association
Pearson	138.51	121.14	0.24
OGK	52.7	48.40	0.21

In Figure 7 (left), the wavenumbers of the FTIR spectra selected by the non-robust and the robust procedures are displayed. For the non-robust method, 79 wavenumbers are selected, and for the robust one 73, with an overlap of 52 non-zero elements in the two linear combinations. The selected wavenumbers between $1860\text{-}1660\text{ cm}^{-1}$ are known to be related to oxidation processes, while wavenumbers between $3651\text{-}3649\text{ cm}^{-1}$ correspond to phenolic antioxidants [Ronai, 2021]. The selected wavenumbers are similar for the non-robust and robust estimators. For the HoG feature vectors, however, a difference in the size of the coefficients can be observed. The coefficient values for the sample covariance are lower, which can be explained by a stronger regularization parameter being chosen during hyperparameter optimization. Note that the coefficients shown in Figure 7b and Figure 7d are normalized such that $b^T C b = 1$. As the HoG features have been extracted from images of wear scar areas, outliers can be expected to be present [cf. Pfeiffer and Filzmoser, 2023]. While such outliers drive the non-robust method towards over-regularization of these features, the robust method based on the OGK estimator reduces the influence of outliers and is able to determine appropriate coefficient values. An example of wear scar images corresponding to outliers identified by the OGK estimator is given in Figure 8.

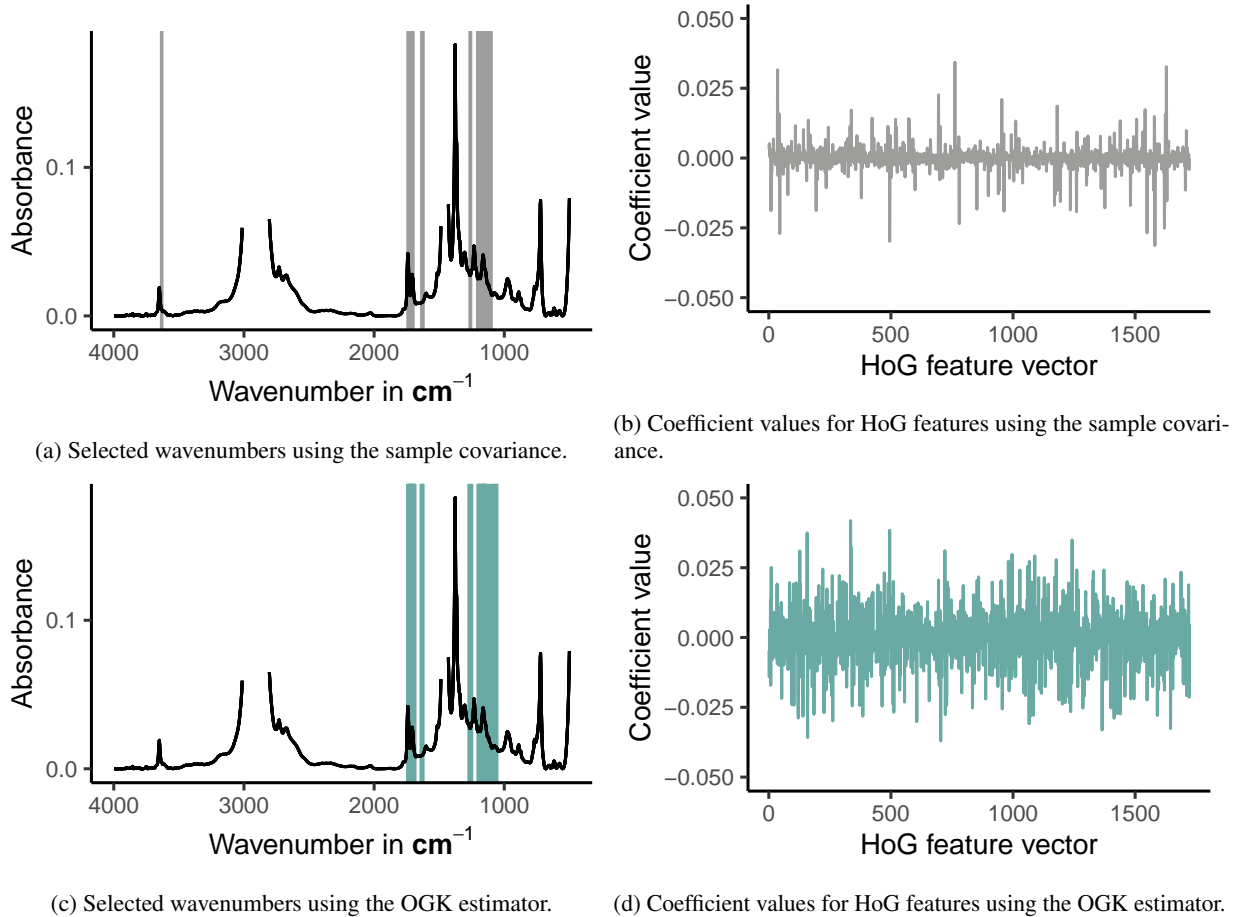


Figure 7: Selected wavenumbers (left) using the sample covariance (top, grey) and the OGK estimator (bottom, green). The plots on the right-hand side show the coefficient vector for the HoG features (classical on top, robust at the bottom). For these, no sparsity penalty was included.

6 Summary and conclusions

We focused on the problem of maximizing the association between linear combinations of two sets of random variables (two multivariate data sets referring to the same observations). If the association measure is taken as the Pearson correlation, this corresponds to the framework of canonical correlation analysis. However, more general association measures can be considered, even allowing for an identification of monotone rather than just linear relationships. The stated problem can also be formulated as a constrained maximization problem, where the joint covariance of the two

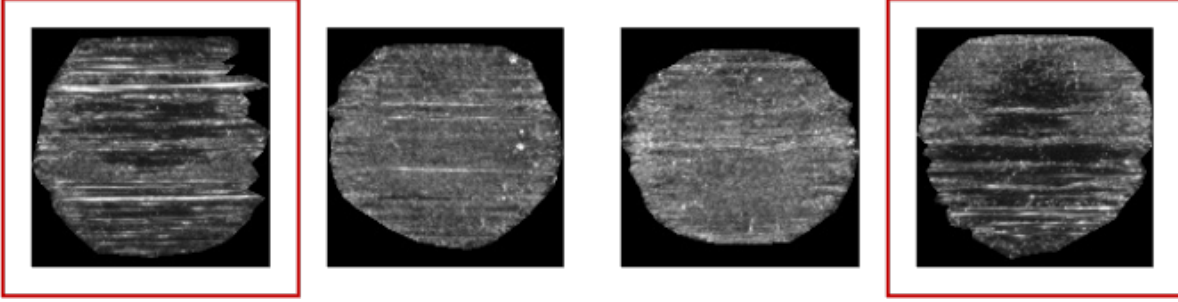


Figure 8: Wear scar areas on the ball for a duration of 552 hours of oil alteration. The framed images correspond to HoG features that were identified as outliers by the OGK estimator.

random variables is involved, and the coefficients for the linear combinations need to be identified. This is the problem considered in this paper, with two extensions: (i) we aim for robustness of the association measure against outliers in one or both data sets, and (ii) we want to have sparsity in one or both vectors of the linear combinations for applications in high dimensions. In this approach, robustness can easily be achieved by plugging in a robustly estimated covariance matrix. Several proposals for this purpose exist in the literature, also for high-dimensional data. We also investigated pairwise estimators of the covariance matrix, e.g., based on Spearman’s rank correlation.

The main contribution of the paper is the development of an efficient algorithm to solve the optimization problem. The formulation in terms of a Lagrange problem makes the use of a gradient descent algorithm possible, where constraints for the linear combinations can easily be incorporated. The minimum requirements for the penalty functions are that they are convex and that (sub)gradients exist. Other than that, the presented algorithm allows flexibility in the choice of penalty functions, and—as seen in one of the examples—also enables to induce sparsity in only one component, while the other is L_2 regularized.

From a computational perspective, the main advantage of our approach is the scalability to a high number of variables. In comparison to solving a regression problem repeatedly [Wilms and Croux, 2015b], or to scanning a larger and larger search space in circles [Alfons et al., 2016b], an algorithm based on gradient descent is more efficient, as only the gradient information needs to be stored. Although the estimation of the plug-in covariance matrix can be computationally demanding, covariance estimation just needs to be done once. This is different from approaches, e.g., based on projection pursuit, where pairwise correlations or association measures need to be computed for all considered projection directions [Alfons et al., 2016b].

We provided numerical results for the precision and theoretical considerations concerning the existence of a solution of the optimization problem. For this, positive definiteness of the joint covariance matrix is a requirement, however, from the simulations we could see that even when this assumption is violated (high-dimensional setting with pairwise estimators), our algorithm is able to produce comparable or even better results than the alternative techniques. The results emphasize how important a good (and robust!) estimator of the covariance is. As the performance regarding robustness and computation time is dependent on the estimator of the covariance matrix, a sparse and robust estimator could lead to improvements. Avella-Medina et al. [2018] show that thresholding methods [see, e.g., Bickel and Levina, 2008] have desirable properties when a robust initial estimator is used. Extending the available implementation to exploit the sparsity structure of the covariance will be explored in our upcoming research.

Examples with high-dimensional data sets from biology and tribology underline the usefulness of our approach: It offers flexibility concerning penalty functions depending on the desired sparsity in each of the data sets, desirable robustness properties and maintains manageable computation times.

The combination of robust estimators and modern optimization techniques yields a powerful toolbox for solving several other common problems in statistics. Especially for robust procedures, where robust estimation (e.g., of a covariance matrix) and optimization can be decoupled, the proposed procedure is very promising. Examples of such extensions are robust principal component analysis and robust linear discriminant analysis, which are topics of our future research.

SUPPLEMENTARY MATERIAL

R-package for Algorithm 1: R-package RobSparseMVA containing code to perform the optimization described in the article, available online <https://github.com/piapfeiffer/RobSparseMVA>.

References

- Pascal GP Martin, Hervé Guillou, Frédéric Lasserre, Sébastien Déjean, Annaig Lan, Jean-Marc Pascussi, Magali SanCristobal, Philippe Legrand, Philippe Besse, and Thierry Pineau. Novel aspects of PPAR α -mediated regulation of lipid and xenobiotic metabolism revealed through a nutrigenomic study. *Hepatology*, 45(3):767–777, 2007.
- R.A. Johnson and D.W. Wichern. *Applied Multivariate Statistical Analysis*. Prentice Hall, Upper Saddle River, 6th edition, 2007.
- Christophe Croux and Catherine Dehon. Analyse canonique basée sur des estimateurs robustes de la matrice de covariance. *La Revue de Statistique Appliquée*, 2, 01 2002.
- Peter J Rousseeuw. Least median of squares regression. *Journal of the American statistical association*, 79(388): 871–880, 1984.
- Peter J Rousseeuw. Multivariate estimation with high breakdown point. *Mathematical statistics and applications*, 8 (283-297):37, 1985.
- Sara Taskinen, Christophe Croux, Annaliisa Kankainen, Esa Ollila, and Hannu Oja. Influence functions and efficiencies of the canonical correlation and vector estimates based on scatter and shape matrices. *Journal of Multivariate Analysis*, 97:359–384, 02 2006. doi:10.1016/j.jmva.2005.03.005.
- Benjamin Langworthy, Rebecca Stephens, John Gilmore, and Jason Fine. Canonical correlation analysis for elliptical copulas. *Journal of Multivariate Analysis*, 183:104715, 12 2020. doi:10.1016/j.jmva.2020.104715.
- Andreas Alfons, Christophe Croux, and Peter Filzmoser. Robust maximum association estimators. *Journal of the American Statistical Association*, 112:1–29, 02 2016a. doi:10.1080/01621459.2016.1148609.
- Andreas Alfons, Christophe Croux, and Peter Filzmoser. Robust maximum association between data sets: the R package ccaPP. *Austrian Journal of Statistics*, 45(1):71–79, 2016b.
- Daniela Witten, Robert Tibshirani, and Trevor Hastie. A penalized matrix decomposition, with applications to sparse principal components and canonical correlation analysis. *Biostatistics (Oxford, England)*, 10:515–34, 05 2009. doi:10.1093/biostatistics/kxp008.
- Mengjie Chen, Chao Gao, Zhao Ren, and Harrison H Zhou. Sparse CCA via precision adjusted iterative thresholding. *arXiv preprint arXiv:1311.6186*, 2013.
- Sandra Waaijenborg, Philip C Verselewe de Witt Hamer, and Aeilko H Zwinderman. Quantifying the association between gene expressions and dna-markers by penalized canonical correlation analysis. *Statistical applications in genetics and molecular biology*, 7(1), 2008.
- Ines Wilms and Christophe Croux. Sparse canonical correlation analysis from a predictive point of view. *SSRN Electronic Journal*, 57, 01 2015a. doi:10.2139/ssrn.2381968.
- Robert Tibshirani. Regression shrinkage and selection via the lasso. *Journal of the Royal Statistical Society Series B: Statistical Methodology*, 58(1):267–288, 1996.
- Andreas Alfons, Christophe Croux, and Sarah Gelper. Sparse least trimmed squares regression for analyzing high-dimensional large data sets. *The Annals of Applied Statistics*, pages 226–248, 2013.
- Xiaolan Gu and Qiusheng Wang. Sparse canonical correlation analysis algorithm with alternating direction method of multipliers. *Communications in Statistics - Simulation and Computation*, 49(9):2372–2388, 2020. doi:10.1080/03610918.2018.1520867.
- Hai Shu, Xiao Wang, and Hongtu Zhu. D-CCA: A decomposition-based canonical correlation analysis for high-dimensional datasets. *Journal of the American Statistical Association*, 115(529):292–306, 2020. doi:10.1080/01621459.2018.1543599.
- Ines Wilms and Christophe Croux. Robust sparse canonical correlation analysis. *BMC Systems Biology*, 10, 01 2015b. doi:10.1186/s12918-016-0317-9.
- Theodore W Anderson. *An introduction to multivariate statistical analysis*. Wiley series in probability and mathematical statistics : Probability and mathematical statistics. Wiley, New York, NY [u.a.], 1958. ISBN 0471026409.
- Kris Boudt, Peter J Rousseeuw, Steven Vanduffel, and Tim Verdonck. The minimum regularized covariance determinant estimator. *Statistics and Computing*, 30(1):113–128, 2020.
- Ricardo A Maronna and Ruben H Zamar. Robust estimates of location and dispersion for high-dimensional datasets. *Technometrics*, 44(4):307–317, 2002.
- Olivier Ledoit and Michael Wolf. A well-conditioned estimator for large-dimensional covariance matrices. *Journal of Multivariate Analysis*, 88(2):365–411, 2004. ISSN 0047-259X. doi:https://doi.org/10.1016/S0047-259X(03)00096-4.

- Valentin Todorov and Peter Filzmoser. An object-oriented framework for robust multivariate analysis. *Journal of Statistical Software*, 32(3):1–47, 2009. doi:10.18637/jss.v032.i03.
- R Core Team. *R: A Language and Environment for Statistical Computing*. R Foundation for Statistical Computing, Vienna, Austria, 2022. URL <https://www.R-project.org/>.
- Ramanathan Gnanadesikan and John R Kettenring. Robust estimates, residuals, and outlier detection with multiresponse data. *Biometrics*, pages 81–124, 1972.
- Victor J Yohai and Ruben H Zamar. High breakdown-point estimates of regression by means of the minimization of an efficient scale. *Journal of the American statistical association*, 83(402):406–413, 1988.
- Christophe Croux and Catherine Dehon. Influence functions of the spearman and kendall correlation measures. *Tilburg University, Center for Economic Research, Discussion Paper*, 19, 01 2010. doi:10.1007/s10260-010-0142-z.
- Peter J Rousseeuw and Geert Molenberghs. Transformation of non positive semidefinite correlation matrices. *Communications in Statistics—Theory and Methods*, 22(4):965–984, 1993.
- Nicholas J Higham. Computing the nearest correlation matrix—a problem from finance. *IMA Journal of Numerical Analysis*, 22(3):329–343, 2002.
- Douglas Bates, Martin Maechler, and Mikael Jagan. *Matrix: Sparse and Dense Matrix Classes and Methods*, 2023. URL <https://CRAN.R-project.org/package=Matrix>. R package version 1.5-4.1.
- Stephen P Boyd and Lieven Vandenberghe. *Convex optimization*. Cambridge University Press, 2004.
- Dimitri P. Bertsekas. *Constrained Optimization and Lagrange Multiplier Methods*. Athena Scientific, Belmont, Massachusetts, 1996. First published by Academic Press, Inc., in 1982.
- Stephen Boyd, Neal Parikh, Eric Chu, Borja Peleato, and Jonathan Eckstein. Distributed optimization and statistical learning via the alternating direction method of multipliers. *Foundations and Trends in Machine Learning*, 3:1–122, 01 2011. doi:10.1561/22000000016.
- Diederik Kingma and Jimmy Ba. Adam: A method for stochastic optimization. In *3rd International Conference on Learning Representations*. ICLR 2015, San Diego, California, May 7 - 9, 2015, 2015.
- S.J. Reddi, S. Kale, and S. Kumar. On the convergence of adam and beyond. In *6th International Conference on Learning Representations*. ICLR 2018, Vancouver, BC, Canada, April 30 - May 3, 2018, 2018.
- Daniel Falbel and Javier Luraschi. *torch: Tensors and Neural Networks with 'GPU' Acceleration*, 2023. <https://torch.mlverse.org/docs>, <https://github.com/mlverse/torch>.
- Peter I Frazier. A tutorial on bayesian optimization. *arXiv preprint arXiv:1807.02811*, 2018.
- Samuel Wilson. *ParBayesianOptimization: Parallel Bayesian Optimization of Hyperparameters*, 2022. URL <https://CRAN.R-project.org/package=ParBayesianOptimization>. R package version 1.2.6.
- Peter Filzmoser, Heinrich Fritz, and Klaudius Kalcher. *pcaPP: Robust PCA by Projection Pursuit*, 2022. URL <https://CRAN.R-project.org/package=pcaPP>. R package version 2.0-3.
- João Branco, Christophe Croux, P Filzmoser, and M. Rosário Oliveira. Robust canonical correlations: A comparative study. *Katholieke Universiteit Leuven, Open Access publications from Katholieke Universiteit Leuven*, 20, 01 2003. doi:10.1007/BF02789700.
- Daniela Witten and Rob Tibshirani. *PMA: Penalized Multivariate Analysis*, 2020. URL <https://CRAN.R-project.org/package=PMA>. R package version 1.2.1.
- Hui Zou, Trevor Hastie, and Robert Tibshirani. Sparse principal component analysis. *Journal of computational and graphical statistics*, 15(2):265–286, 2006.
- Valentin Todorov and Peter Filzmoser. Comparing classical and robust sparse pca. In *Synergies of soft computing and statistics for intelligent data analysis*, pages 283–291. Springer, 2013.
- Ignacio González and Sébastien Déjean. *CCA: Canonical Correlation Analysis*, 2021. URL <https://CRAN.R-project.org/package=CCA>. R package version 1.2.1.
- Pia Pfeiffer, Bettina Ronai, Georg Vorlaufer, Nicole Dörr, and Peter Filzmoser. Weighted LASSO variable selection for the analysis of ftir spectra applied to the prediction of engine oil degradation. *Chemometrics and Intelligent Laboratory Systems*, 228:104617, 2022.
- Pia Pfeiffer and Peter Filzmoser. Robust statistical methods for high-dimensional data, with applications in tribology. *Analytica Chimica Acta*, page 341762, 2023. ISSN 0003-2670. doi:<https://doi.org/10.1016/j.aca.2023.341762>. URL <https://www.sciencedirect.com/science/article/pii/S0003267023009832>.

-
- Bettina Ronai. Evaluation of chemical and tribometrical data of engine oils by selected multivariate statistics. Master's thesis, TU Wien, 2021.
- Marco Avella-Medina, Heather S Battey, Jianqing Fan, and Qiefeng Li. Robust estimation of high-dimensional covariance and precision matrices. *Biometrika*, 105(2):271–284, 2018.
- Peter J. Bickel and Elizaveta Levina. Covariance regularization by thresholding. *The Annals of Statistics*, 36(6):2577 – 2604, 2008. doi:10.1214/08-AOS600. URL <https://doi.org/10.1214/08-AOS600>.